Monatsh Chem (2010) 141:157–168
DOI 10.1007/s00706-009-0235-2

ORIGINAL PAPER

A new dioxotetraamine ligand derived from binicotinic acid: synthesis, coordination, and fluorescence behaviour towards divalent transition metal ions

Bikram Kishore Kanungo · Minati Baral · Rati Kanta Bera · Suban Kumar Sahoo

Received: 17 September 2008 / Accepted: 27 November 2009 / Published online: 9 January 2010

Abstract A novel bipyridyl-based fluorescent system, *N*,*N*′-bis(2-aminoethyl)-2,2′-bipyridine-3,3′-dicarboxamide (BABD), with two different coordination sites, bidentate bipyridyl and tetradentate dioxotetraamine, has been synthesized, and characterized by elemental analysis and spectroscopic (UV–Vis, IR, ^{1}H NMR, and ^{13}C NMR) methods. The lowest energy molecular geometry of BABD was obtained by empirical then quantum mechanical treatment. The binding ability of BABD with H^{+}, Co(II), Ni(II), Cu(II), and Zn(II) ions was investigated in aqueous 0.1 M KCl at 25 ± 1 °C by potentiometric methods. Four protonation constants were determined for BABD, and were used as input data to evaluate the formation constants of the metal complexes. The coordination behaviour of BABD in solution indicated that at low pH the bipyridyl unit coordinates to all metal ions, but at higher pH (>7.0) coordination of the dioxotetraamine unit occurs with the Cu(II) and Ni(II) ions only. The 3D-model structure of the metal complex was predicted by semi-empirical calculation using the AM1/d Hamiltonian. Fluorimetric titrations indicate that at pH 9 BABD exhibits fluorescence enhancement with increasing concentration of Cu(II) and Ni(II) ions, but at pH 7.2 fluorescence enhancement is observed only in the presence of Cu(II) ions. No remarkable effect on the fluorescence of BABD was observed in the presence of other biologically relevant metal ions, for example Ni(II), Fe(II), Mn(II), Co(II), Zn(II), Mg(II), Ca(II), and Hg(II).

Keywords Semi-empirical calculations · Sensor · Metal complexes · Copper · Stability constants

B. K. Kanungo (✉) · R. K. Bera
Department of Chemistry, Sant Longowal Institute of Engineering and Technology, Longowal 148 106, Punjab, India
e-mail: b.kanungo@vsnl.com

M. Baral
Department of Chemistry, National Institute of Technology, Kurukshetra 136 119, Haryana, India

S. K. Sahoo
Department of Chemistry, S V National Institute of Technology, Surat, India

Introduction

In recent years there has been burgeoning interest in the design of chelating agents which can selectively bind metal ions of interest [1–4]. The design of such chelates received widespread stimulation in the late 1970s [5, 6] after the development of supramolecular chemistry and the pioneering work of Pedersen, Cram, and Lehn. Whenever such a chelate is suitably linked to a light-emitting group (fluorophore) through a spacer, it produces a distinct fluorescence signal on chelation with the metal ion (analyte). This signal is helpful for both qualitative and quantitative estimation of the target metal ion for which the chelate is designed. During analyte detection, the fluorosensor undergoes two processes, i.e. molecular recognition and signal transduction, which can be understood schematically from Scheme 1 representing an ON–OFF fluorosensor. In an ON–OFF fluorosensor, complete fluorescence of the fluorophore is observed when no analyte is bound to the receptor. Once the analyte is recognized by the receptor, fluorescence is quenched, presumably because of either electron-transfer (eT) or energy-transfer (ET) processes [7, 8]. Besides quenching, fluorescence enhancement of the fluorophore is also implemented in the design of fluorosensors [9–14].

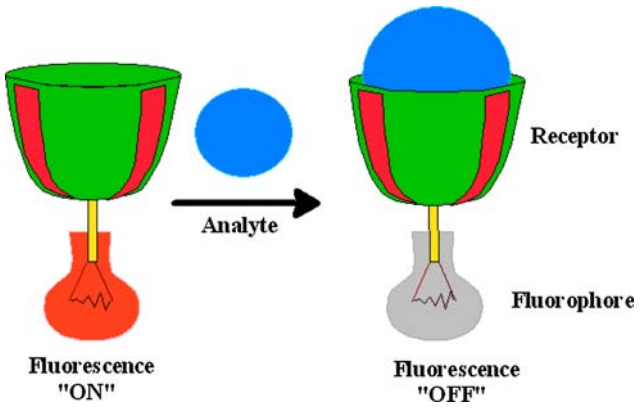

Scheme 1

In designing fluorescent metal ion sensors, the receptor chosen must have selective and efficient metal ion-binding ability. Dioxotetraamine ligands are widely implemented in the design of various molecular devices because of their fascinating coordination behaviour [15]. In dioxotetraamines, the metal ion coordinates through two deprotonated amide N-atoms and two amine N-atoms to form a square-planar N_4 complex [16]. Analysis of the solid-state structures of their metal complexes reveals that the metal–N(amide) bond length is somewhat shorter than the corresponding metal–N(amine) bond length [17, 18]. This effect is ascribed mainly to the strong σ-donor properties of the deprotonated amide groups and helps, to some extent, to provide extra stabilization [19]. Solution studies indicate that the coordination of dioxo-amides is pH dependent. In acidic media, the ligand coordinates only through amine nitrogen atoms whereas in basic or slightly acidic media, amide N-atoms and amine N-atoms coordinate upon deprotonation as anions (Fig. 1a) [18, 20]. The pH-dependent, selective, and efficient metal ion-binding abilities of dioxotetraamines stimulated the idea of designing molecular devices such as cation-selective fluorosensors (Fig. 1a) [21–29], and multi-component systems in which a metal ion can be translocated with the change in pH (Fig. 1b) [30–34]. The importance of dioxotetraamines is also related with their:

1 dual structural features of tetraamine and oligopeptide;
2 potential to stabilize anomalously high oxidation states (e.g. Ni(III) and Cu(III)) in aqueous media [35–37]; and

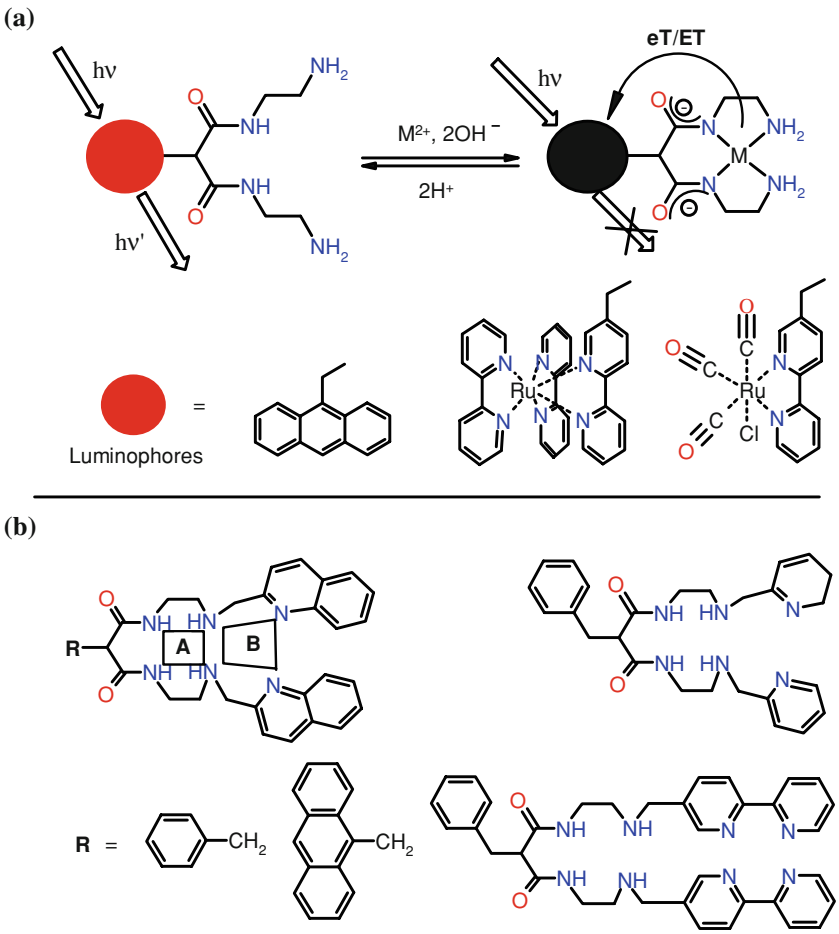

Fig. 1 **a** Schematic representation of metal ion coordination in dioxotetraamines, and some cation-selective fluorescent sensors (*eT* electron transfer, *ET* energy transfer); **b** dioxotetraamine-based ditopic ligands designed for pH-driven translocation of divalent transition metal ions

3 implementation as model compounds to elucidate the reactivity of superoxide dismutase (SOD) etc. [38].

Bipyridyl and its derivatives are known to be excellent chelators for transition metal ions and have been exploited in the development of supramolecular devices [39–42].

Keeping the above facts in view, herein we have introduced a new water-soluble chelator *N*,*N*′-bis(2-aminoethyl)-2,2′-bipyridine-3,3′-dicarboxamide (BABD) with two different coordination sites, i.e. bipyridyl and dioxotetraamine units. The coordination behaviour of BABD with the metal ions Co(II), Ni(II), Cu(II), and Zn(II) has been investigated by pH–potentiometric methods at an ionic strength of 0.1 M KCl at 25 ± 1 °C. The formation constants of the various complexes formed in solution and their selectivity towards the metal ions are reported. The 3D-model structures of the metal complexes depicted in solution were predicted by means of molecular modelling calculations. Fluorimetric titration was carried out in presence of various biologically relevant metal ions in order to explore BABD as a cation-selective fluorescence sensor.

Results and discussion

Synthesis of the ligand

The ligand BABD was synthesized as shown in Scheme 2 by reacting an ester of binicotinic acid with freshly distilled ethylenediamine. It was characterized by elemental analysis and use of a variety of spectroscopic (UV–Vis, IR, ^{1}H NMR, and ^{13}C NMR) methods. The ligand is soluble in water, methanol, and ethanol but insoluble in the common organic solvents chloroform, dichloromethane, and THF.

The ligand in aqueous medium has two peaks at 212 and 261 nm attributed to $\pi \rightarrow \pi^*$ transitions associated with the chromophoric bipyridyl ring. The calculated electronic spectrum of BABD obtained from a PM3 (RHF) optimized structure by employing the semi-empirical ZINDO method showed peaks with λ_{max} at 236 and 280 nm. The optimized structure of BABD and the HOMO and LUMO molecular orbital diagrams at 280 nm are shown in Fig. 2.

The infrared spectra of BABD contained a band at 3,350 cm^{-1}, characteristic of ν_{N-H}. A broad band at 3,426 cm^{-1} was observed for ν_{N-H} (amine) and

Scheme 2

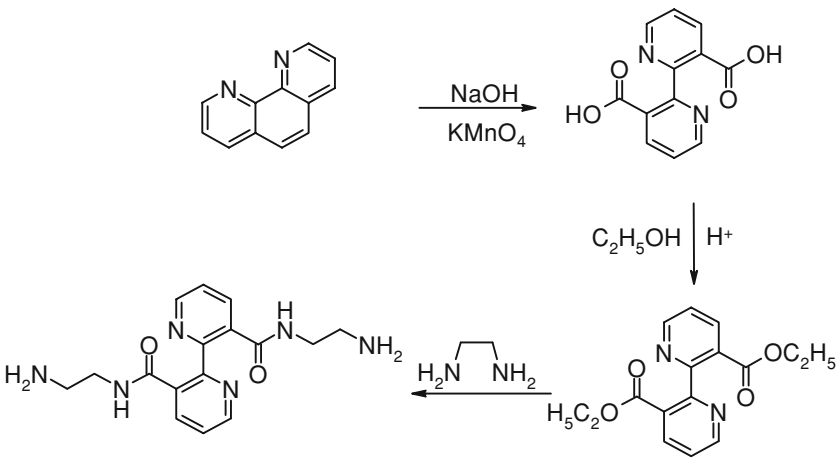

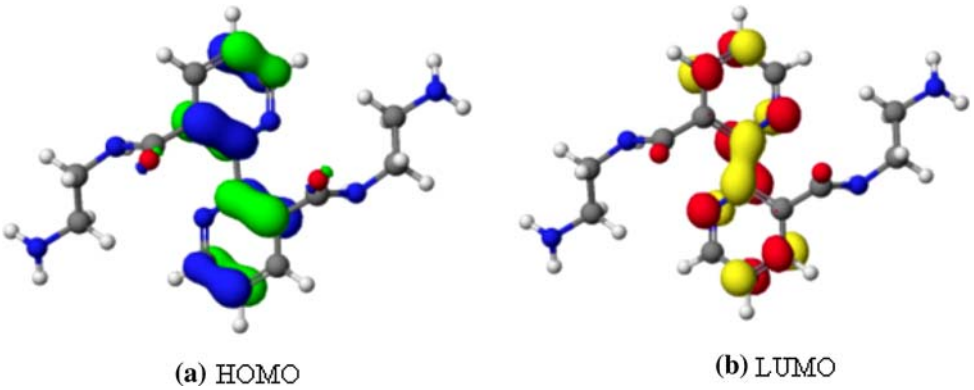

Fig. 2 HOMO (**a**) and LUMO (**b**) molecular orbital diagrams of the ligand BABD at λ_{max} = 280 nm obtained by applying the semi-empirical PM3/ZINDO method

presumably also due to the ν_{N-H} (2° amide). The characteristic amide I and II $\nu_{C=O}$ bands were observed at 1,652 and 1,578 cm^{-1}, respectively. The band 1,578 cm^{-1} is possibly also due to the bending vibration of the amine group (δ_{NH}). The amide III ν_{C-N} and δ_{N-H} for BABD were observed at 1,242 and 796 cm^{-1}, respectively.

The ^{1}H NMR spectrum of the ligand showed three dd signals at 7.5, 8.0, and 8.6 ppm, characteristic of aromatic protons. Two triplets centred at 3.1 and 2.5 ppm are assigned for the methylene groups linked to the amide and amine groups, respectively. No peak was observed for amine and amide protons, which may be because of deuterium exchange. The ^{13}C NMR spectrum of BABD contained peaks at 39.65 and 42.21 ppm for CH_2 groups attached to the amine and amide groups, whereas the peaks at 124.49, 131.38, 137.14, 150.04, and 154.16 ppm are attributed to aromatic carbons. The peak at 169.72 ppm corresponds to the amide carbonyl carbon.

Ligand protonation constants

The protonation constants of the ligand were determined by potentiometric and spectrophotometric methods. For the potentiometric method the acidified ligand solution was titrated against standard KOH at an ionic strength of 0.1 M KCl and 25 ± 1 °C in aqueous medium. Analysis of potentiometric curve (Fig. 3) of the ligand BABD with the computer software Hyperquad 2000 gave four protonation constants: 8.89 ± 0.04, 8.41 ± 0.03, 3.54 ± 0.09, and 2.68 ± 0.07.

The equilibrium reactions for these protonation constants are given by the equations:

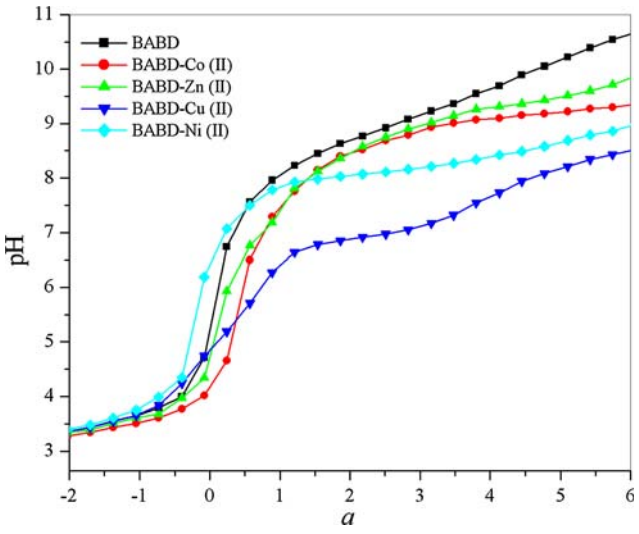

Fig. 3 Potentiometric titration curves of BABD in the absence and presence of the metal ions Co(II), Ni(II), Cu(II), and Zn(II) in 1:1 ligand–metal molar ratio, where "*a*" is moles of base added per mole of ligand present

$$LH_{n-1} + H^{+} \rightleftharpoons LH_n \quad K_n = \frac{[LH_n]}{[LH_{n-1}][H^{+}]} \tag{1}$$

The first two protonation constants of BABD are similar to that obtained for dioxotetraamine (log $K = 9.6$ and 8.3 [21]), and can be assigned to the protonation of two amine groups, whereas the other two values are because of the protonation of bipyridyl N-atoms of BABD (for a non-substituted bipyridyl log $K = 4.34$ and 1.46 [43]). This is again supported by the fact that bipyridyl nitrogens are generally characterized by far lower basicity than amine nitrogens. The amide group requires strongly basic conditions for deprotonation, thus it was not possible to determine the protonation constants of the amide groups under the experimental conditions used. The two protonation constants of the ligand assigned to bipyridyl nitrogens, with $\Delta\log K = 0.86$, can be attributed to the change in the electronic environment of the ligand after uptake of one proton.

The pH dependent species distribution of BABD (Fig. 4) indicates that the ligand exists in different protonated forms between pH ~2 and ~11. Completion of the deprotonation of the bipyridyl groups was observed in steps, forming LH_3 and LH_2 species at pH < ~6. As the pH increases, two amine nitrogen atoms are deprotonated stepwise to form LH and the neutral species L, which is predominant above pH 9.5.

Spectrophotometric titration of the ligand BABD was also carried out in aqueous solution in acidic and basic media to explain the deprotonation process. The spectra were recorded in the region 200–380 nm, and in the pH range 2.54–9.83. The state of equilibrium between the protonated and deprotonated ligand can be examined

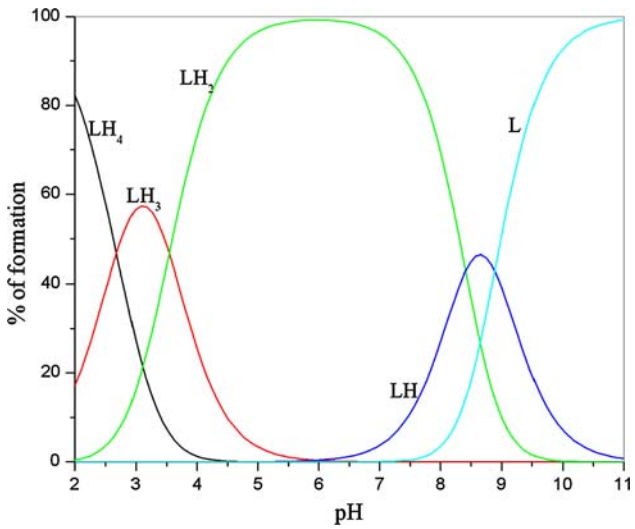

Fig. 4 pH-dependent species distribution curve for BABD

from the formation of isosbestic points (Fig. 5). Analysis of experimental data by global fitting of the whole spectral data (Fig. 5) using the software pHAb gave four protonation constants: 8.81 ± 0.05, 8.35 ± 0.04, 3.47 ± 0.03, and 2.71 ± 0.05. The four protonation constants obtained from the spectrophotometric method agree with the results obtained from the potentiometric method. The protonated ligands in this investigation gave two peaks at about 272 and 217 nm which correspond to band-I and band-II $\pi \rightarrow \pi^*$ transitions of the aromatic ring. Deprotonation caused a bathochromic shift in band-I of the absorption bands and an increase in the absorbance of band-II. In order to verify the validity and assignments of the experimental protonation constants, aqueous-phase free energy for the entire representative species was calculated using the semi-empirical PM3/COSMO quantum mechanical approach [44]. The acidity of a base BH, i.e. the pK_a, defined as the negative logarithm of the dissociation constant of the reaction $BH + H_2O = B + H_3O^+$, is given by the thermodynamics relationship $pK_a = \Delta G_{aq,BH}/2.303RT$. For BABD, the change in aqueous phase free energy was obtained by use of the equations:

$$\Delta G_{aq,BH_4} = \left(G_{aq,BH_3} + G_{aq,H_3O^+}\right) - \left(G_{aq,BH_4} + G_{aq,H_2O}\right) \quad (2)$$

$$\Delta G_{aq,BH_3} = \left(G_{aq,BH_2} + G_{aq,H_3O^+}\right) - \left(G_{aq,BH_3} + G_{aq,H_2O}\right) \quad (3)$$

$$\Delta G_{aq,BH_2} = \left(G_{aq,BH} + G_{aq,H_3O^+}\right) - \left(G_{aq,BH_2} + G_{aq,H_2O}\right) \quad (4)$$

$$\Delta G_{aq,BH} = \left(G_{aq,B} + G_{aq,H_3O^+}\right) - \left(G_{aq,BH} + G_{aq,H_2O}\right) \quad (5)$$

The group with the greater acidity is that for which hydrogen release is easier and there must be a decrease in ΔG values in the deprotonation process. A clear decrease in ΔG was observed in the case of BABD (Fig. 6), because deprotonation of the fully protonated free ligand LH_4 took place first from bipyridyl N-atoms followed by protonated amines. The validity of this calculated ΔG_{aq} for the different species of BABD was compared with the experimental pK_a, which resulted an acceptable correlation with $R = 0.98522$.

Metal complexes

The potentiometric titration of ligand BABD (L) in the presence of the metal ions Co(II), Ni(II), Cu(II), and Zn(II) was carried out at an ionic strength of $\mu = 0.1$ M KCl and 25 ± 1 °C by keeping the metal-to-ligand molar ratio 1:1 and 2:1 in aqueous medium. The titration curves for all the metal–ligand systems and that for the free ligand are shown in Figs. 3 and 7 for the 1:1 and 2:1 systems, respectively. The deviations of the metal–ligand titration curves from the free ligand curve indicate the formation of metal complexes. No M_2L complex formation was observed in the reaction mixture of 2:1 metal-to-ligand molar ratio for Co(II) and Zn(II), and hence the titration curves for the 1:1 ratio are presented for these two metal ions only. Ligand BABD formed dinuclear complexes with Ni(II) and Cu(II). The dinuclear species are only prevalent in solution when the metal-to-ligand ratio is 2:1, whereas such species do not exist in solution when the metal-to-ligand molar ratio is maintained at 1:1.

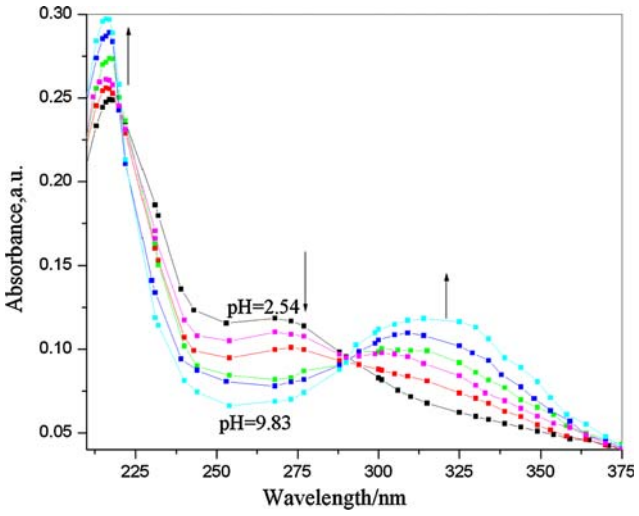

Fig. 5 Electronic spectra of BABD as a function of pH (2.54–9.83) during a spectrophotometric titration. [BABD] = 0.05 mM, [KCl] = 0.1 M and $T = 25 \pm 1$ °C

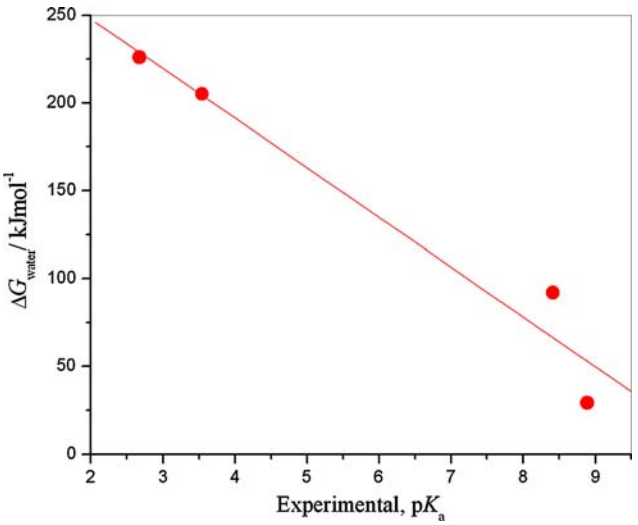

Fig. 6 Correlation between experimental pK_a and calculated free energy ΔG_{aq}

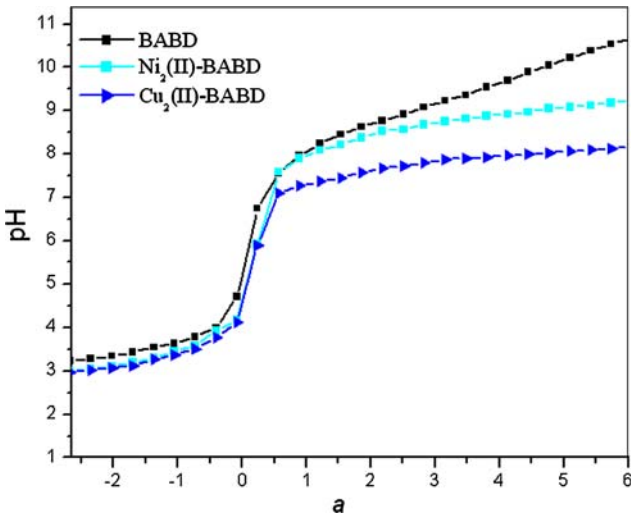

Fig. 7 Potentiometric titration curves of BABD in the absence and presence of metal ions Ni(II) and Cu(II) in 2:1 metal-to-ligand molar ratio, where "*a*" is moles of base added per mole of ligand present

Mononuclear complexes

Analyses of the potentiometric curves using the computer software Hyperquad 2000 enabled the determination of various metal complex species in equilibrium; their formation constants are summarized in Table 1. Ligand BABD forms mononuclear complexes with Co(II), Ni(II), Cu(II), and Zn(II). The best-fit models include MLH_2 and MLH for Co(II) and Zn(II); and MLH_2, MLH, MLH_{-1}, and MLH_{-2} for Cu(II) and Ni(II). In addition to these models, Cu(II) also formed the ML species. Formation of the different species from the best-fit model can be represented by the equations:

$$M + L + 2H \rightleftharpoons MLH_2 \quad \log \beta_{MLH_2} = \frac{[MLH_2]}{[M][L][H]^2} \tag{6}$$

$$M + L + H \rightleftharpoons MLH \quad \log \beta_{MLH} = \frac{[MLH]}{[M][L][H]} \tag{7}$$

$$M + L \rightleftharpoons ML \quad \log \beta_{ML} = \frac{[ML]}{[M][L]} \tag{8}$$

$$ML \rightleftharpoons MLH_{-1} + H \quad \log \beta_{MLH_{-1}} = \frac{[MLH_{-1}][H]}{[ML]} \tag{9}$$

$$MLH_{-1} \rightleftharpoons MLH_{-2} + H \quad \log \beta_{MLH_{-2}} = \frac{[MLH_{-2}][H]}{[MLH_{-1}]} \tag{10}$$

The solution species distribution curves (Fig. 8) indicate that complexation occurs from pH ~2. The ligand, which initially exists in the fully protonated form (LH_4), starts to deprotonate with the formation of MLH_2 species. Formation of MLH_2 species takes place with the release of two protons from the fully protonated ligand LH_4 and also, presumably, because of the coordination of deprotonated bipyridyl N-atoms (Fig. 9a). Subsequent release of protons from MLH_2 led to the formation of MLH and ML (ML was depicted only in the Cu(II)–BABD system). These protons from MLH_2 are released in steps from the two protonated amine groups. Therefore the formation of MLH and ML can be explained in two ways:

1 the metal ion coordinated to the bipyridyl unit may translocate towards the dioxotetraamine unit with the stepwise deprotonation and coordinate to the amine N-atoms; or
2 protonated amines release protons with the rise in pH without any interaction with the metal ion.

The formation, by BABD–Cu/Ni systems, of species of the types MLH_{-1} and MLH_{-2} in slightly basic media indicate the deprotonation and coordination of amide N-atoms. This is possible only if the metal ion is translocated from bipyridyl to the dioxotetraamine unit. Accordingly, pH-driven translocation of the metal ion can be accepted in the BABD system and the proposed coordination modes for ML and MLH_{-2} can be represented by Fig. 9b, c. The pH-driven translocations of the metal ion in dioxotetraamine-derived ligands have been well documented by Fabrrizzi and his coworkers [30–34].

The coordination of amide groups was observed only for BABD–Cu(II) and BABD–Ni(II) systems from pH ~7.1 to ~8.1 (Fig. 8) whereas no such species formation (MLH_{-1}

Table 1 Formation constants (log β) of various metal complexes formed by ligand BABD at 25 ± 1 °C and μ = 0.1 M KCl

Reactions	Co(II)	Ni(II)	Cu(II)	Zn(II)
$M + L + 2H \rightleftharpoons MLH_2$	18.8 ± 0.10	19.52 ± 0.02	20.05 ± 0.07	18.80 ± 0.0
$M + L + H \rightleftharpoons MLH$	13.37 ± 0.08	13.47 ± 0.07	13.54 ± 0.03	13.35 ± 0.08
$M + L \rightleftharpoons ML$	–	–	6.98 ± 0.07	–
$ML \rightleftharpoons M\,LH_{-1} + H$	–	−4.05 ± 0.03	−1.62 ± 0.04	–
$MLH_{-1} \rightleftharpoons MLH_{-2} + H$	–	−3.37 ± 0.07	−9.93 ± 0.05	–
$2\,M + L \rightleftharpoons M_2L$	–	19.67 ± 0.03	20.33 ± 0.10	–
$M_2L \rightleftharpoons M_2LH_{-2} + 2H$	–	1.32 ± 0.08	4.24 ± 0.1	–

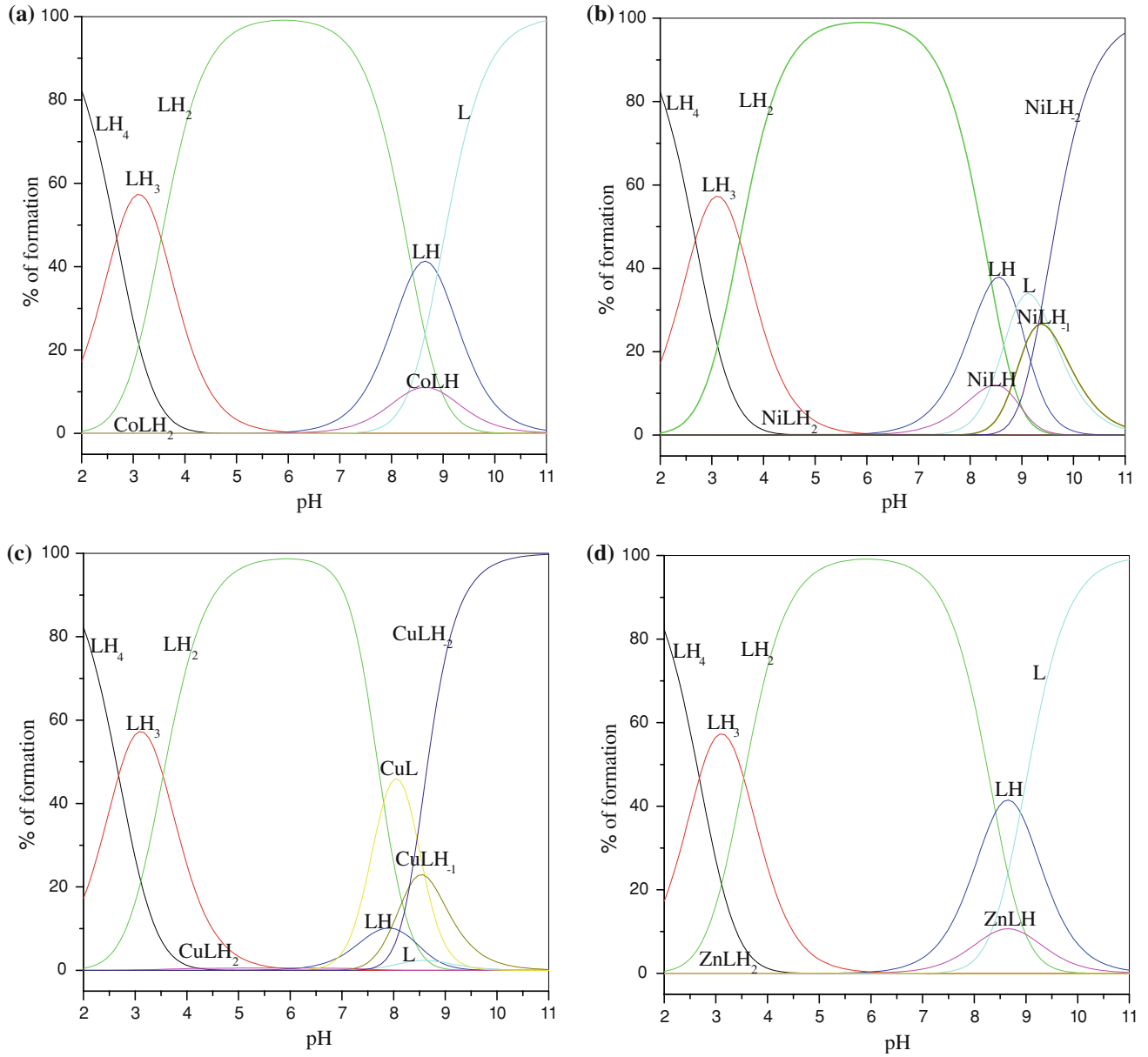

Fig. 8 Species distribution curves for the mononuclear metal complexes **a** Co–BABD, **b** Ni–BABD, **c** Cu–BABD, and **d** Zn–BABD

Fig. 9 Proposed modes of coordination of BABD in the metal complexes in solution (coordination of water molecule not shown)

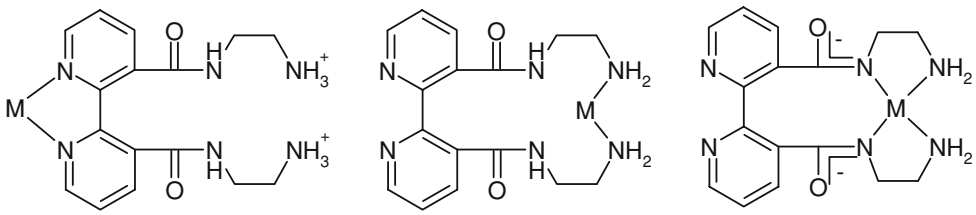

(a) MLH_2 **(b)** ML **(c)** MLH_{-2}

and MLH_{-2}) due to amide deprotonation and coordination was observed for the Zn(II) and Co(II) ions.

This discrepancy is because deprotonation of the amide group is very endothermic and can take place if it is compensated energetically by the formation of a strong bond between the metal and the deprotonated amide group [19]. This is the case for the Cu(II) and Ni(II) ions, which profit greatly from ligand field stabilization effects,

whereas Co(II) and Zn(II) ions do not profit much from ligand field effects and thus do not promote much deprotonation of amide groups [19].

Further MLH_{-1} and MLH_{-2} species detected for Cu(II) and Ni(II) complexes are not hydroxo species; this is evident from the stability factors also. Stepwise deprotonation of the amide group in the ligand leads to the formation of these two types of complexes. It is well documented in the literature that deprotonation of amide protons and chelation with Cu(II) and Ni(II) lead to the formation of square planar complexes [25–28].

Considering the above experimental evidence on the coordination modes of ligand BABD, it may be inferred that coordination to all the metal ions occurs first through two bipyridyl N-atoms at low pH. As the pH increases, deprotonation and coordination of two amide groups take place only in Ni(II) and Cu(II) systems, in which the ligand BABD coordinates through two N-amide and two N-amine groups. The probable structures of the Cu(BABD) and Ni(BABD) complexes in solution were predicted by the semi-empirical AM1/d method. The AM1/d Hamiltonian was chosen for the calculations because of its parameterization for these metal ions and because of its satisfactory prediction of the molecular structure of metal complexes [45]. First, the energetically least strained structures for the metal complexes were obtained by the molecular mechanics MM3 method; these were then further re-optimized by applying the semi-empirical AM1/d method. The optimized structure for the Cu(BABD) complex (Fig. 10) predicted a distorted square planar geometry, which was greatly stabilized by the electrostatic interaction between the positively charged copper ion and the formally negatively charged amide groups. The calculated bond lengths for Cu(BABD) and Ni(BABD), Cu–N(amine) 2.083 Å, Ni–N(amine) 2.508 Å, Cu–N(amide) 1.959 Å, and Ni–N(amide) 2.323 Å, indicate that the deprotonated amide nitrogen atoms coordinate with shorter bond length than the corresponding amine nitrogen atoms; this is in good agreement with previously reported bond lengths for similar ligands obtained by use of single-crystal X-ray diffraction techniques [46–48].

Dinuclear complexes

Analysis of potentiometric data obtained for 2:1 metal-to-ligand molar ratios using the software Hyperquad gave the best fit for the models M_2L and M_2LH_{-2} for both Ni(II) and Cu(II). The formation of the various species from the best-fit model can be represented by the equations:

$$2M + L \rightleftharpoons M_2L \quad \log \beta_{M_2L} = \frac{[M_2L]}{[M]^2[L]} \tag{11}$$

$$M_2L \rightleftharpoons M_2LH_{-2} + 2H \quad \log \beta_{M_2LH_{-2}} = \frac{[M_2LH_{-2}][H]^2}{[M_2L]} \tag{12}$$

From the species distribution curves shown in Fig. 11a and b, it is clear that the M_2L species reaches its maximum concentration at pH 7.5 and 8.5 for Cu(II) and Ni(II) ions, whereas at $pH > 9.5$ and $pH > 10.5$ the deprotonated complexes $[Cu_2LH_{-2}]$ and $[Ni_2LH_{-2}]$ are the predominant species. Theoretically two structures can be proposed for the M_2L type of complex: one with coordination of two bipyridyl sites with one metal ion while the other metal ion binds to two amine N atoms (Fig. 12a). The other structure is shown in Fig. 12b; in this each metal ion binds to one bipyridyl N and to one amine nitrogen atom, assuming the remaining coordination sites are occupied by water molecules. The structure represented in Fig. 12b is more feasible, because in the free ligand the two bipyridyl nitrogens and the pendant arm are expected to remain away from each other because of steric repulsion and the metal ion can coordinate without a conformational change in the ligand. Also, molecular mechanics calculations using the

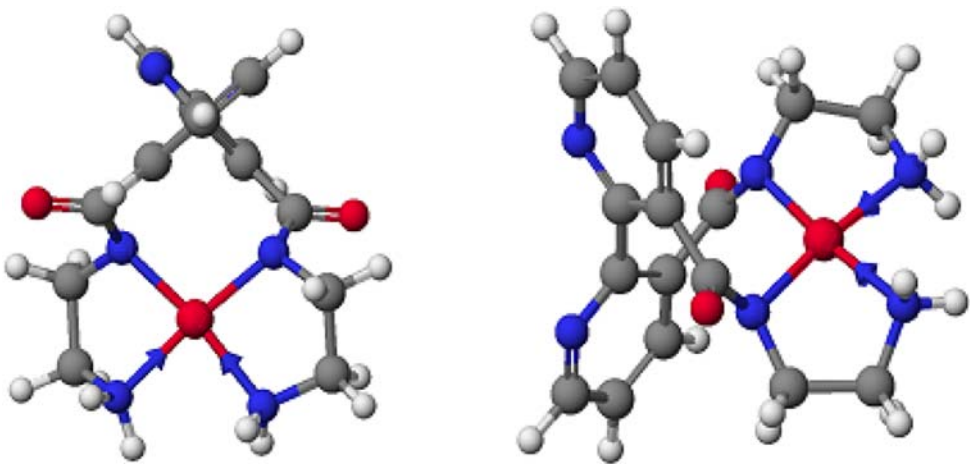

Fig. 10 Two views of the optimized structure of Cu(BABD) obtained by the semi-empirical AM1/d method

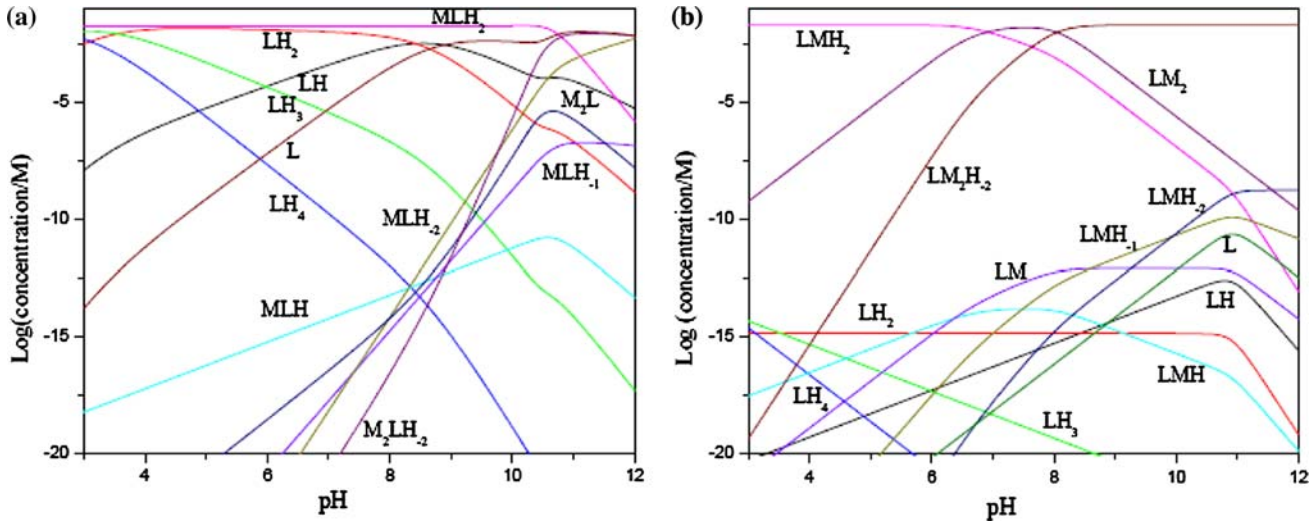

Fig. 11 Species distribution curves for the dinuclear metal complexes **a** Ni–BABD and **b** Cu–BABD

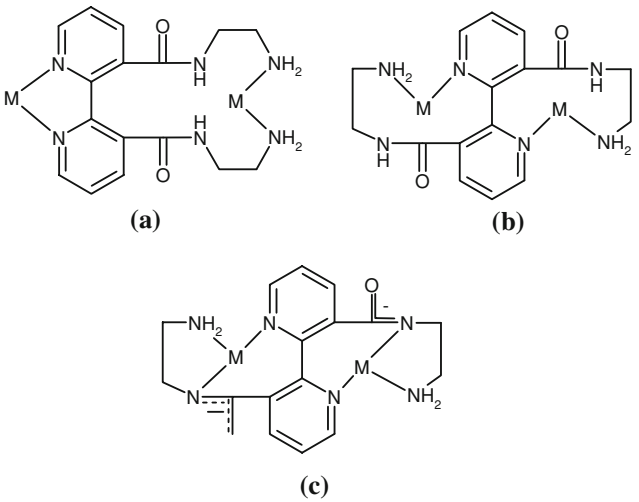

Fig. 12 Proposed coordination modes of dimeric metal complexes of BABD in solution (coordination of water molecule not shown)

MM+ force field were used to obtain the energetically most favorable structure. The calculated strain energy of the structure presented in Fig. 12a was 281.3 kJ/mol higher than that of the structure in Fig. 12b. As the pH is increased further, deprotonation of amide groups takes place and the amide N-atoms coordinate as anions to the metal ions, in addition to the already coordinated amine N-atoms, replacing one of the coordinated water molecules. This leads to the formation of the species M_2LH_{-2}; the proposed structure is shown Fig. 12c. For comparison, molecular mechanics calculations of this structure and that derived from the structure in Fig. 12a were also carried out. The calculated strain energy reveals that the structure in Fig. 12c is energetically more favourable and is 48.86 kJ/mol less than the other. Similar work, by X-ray crystal analysis, on dinuclear Pd(II) compounds with the ligand bearing bipyridine and carbamoyl groups has recently been reported by Kim et al. [39].

Fluorescence studies

The ligand BABD in aqueous medium ($c_L \leq 10^{-6}$ M) showed good photo-stability on exposure to UV light at room temperature. It does not undergo any kind of decomposition. Also, the emitting behavior of BABD ($\lambda_{ex} = 283$ nm) over the pH range 2–11 was investigated by fluorimetric titration. At low pH the ligand BABD in its fully protonated form showed very poor emission at 379 nm. As the deprotonation occurred from bipyridyl and amine N-atoms with increasing pH, the fluorescent intensity (I_f) of BABD increases steeply and remains constant after pH $\sim$9.0.

The fluorescence efficiency of BABD was also estimated by measuring its fluorescent quantum yield (ϕ) using Eq. (13) (anthracene was used as standard).

$$\phi_u = \phi_{st}\frac{S_u}{S_{st}}\frac{A_{st}}{A_u}\frac{\eta_u^2}{\eta_{st}^2} \tag{13}$$

ϕ_u and ϕ_{st} are the emission quantum yield of the sample and standard, respectively. A_{st} and A_u are the absorbance of the standard and sample, S_{st} and S_u are integrated emission band areas of the standard and samples, and η_{st} and η_u are the solvent refractive indices of the standard and sample, respectively. The calculated ϕ for BABD was found to be 0.06.

The fluorimetric titrations of BABD at 10^{-6} M were carried out in the presence of various divalent metal ions, for example cobalt, nickel, copper, zinc, calcium, and magnesium, at pH 9.0. No noticeable change in the fluorescent properties of the ligand was observed except for the

Cu(II) and Ni(II) ions. In the presence of Cu(II) and Ni(II) ions, the fluorescence intensity of BABD was enhanced appreciably (Fig. 13). The I_f enhancement may be because of the ability of Cu(II) and Ni(II) ions to undergo chelation with the dioxotetraamine unit. Iyer and group also reported fluorescence enhancement on addition of Ni(II) ion to a carboxyphenyltriazine-based system [49]. Recently a few sensors have been reported in which binding of Cu(II) caused an increase in the fluorescence emission [50–52]. Furthermore, to evaluate the potential application and efficiency of BABD as fluorescence sensor, competition experiments were carried out at the same pH and concentration and in the presence of other metal ions. The results show that BABD on complexation with Cu(II) and Ni(II) at pH 9 did not change significantly in the presence of the transition metal ions Mn(II), Co(II), Zn(II), Cd(II), and Hg(II) at concentrations up to 25 $\times$ 10^{-6} M. Furthermore, large excesses of the metal ions Li(I), Na(I), K(I), Mg(II), and Ca(II) did not interfere with detection of Cu(II) and Ni(II). The different chelating abilities (higher for Cu(II) than for Ni(II)) can also enable one to distinguish between them, because complexation of the dioxotetraamine unit of BABD with Cu(II) takes place at lower pH (pH 7.1) than for Ni(II) (pH 8.1) (Fig. 8). Thus, detection of the desired metal ion (Cu(II) or Ni(II)) is possible if one operates at the proper pH. The presence of Cu(II) ions interferes with detection of Ni(II) ions, however. Spectrofluorimetric study of BABD (Fig. 14) at pH 7.2 showed no variation in fluorescence intensity on addition of Ni(II), whereas addition of Cu(II) caused fluorescence enhancement. At pH 7.2, therefore, the sensor BABD recognizes Cu(II) but not Ni(II). Other metal ions (Fe(II), Mn(II), Co(II), Zn(II), Mg(II), Ca(II), and Hg(II)) were also tested at pH 7.2 and 9.0 (Fig. 14) but no noticeable change in the fluorescent intensity was observed. Thus, BABD can be implemented as a potential fluorescent sensor for Cu(II) ions at pH $\sim$7.2.

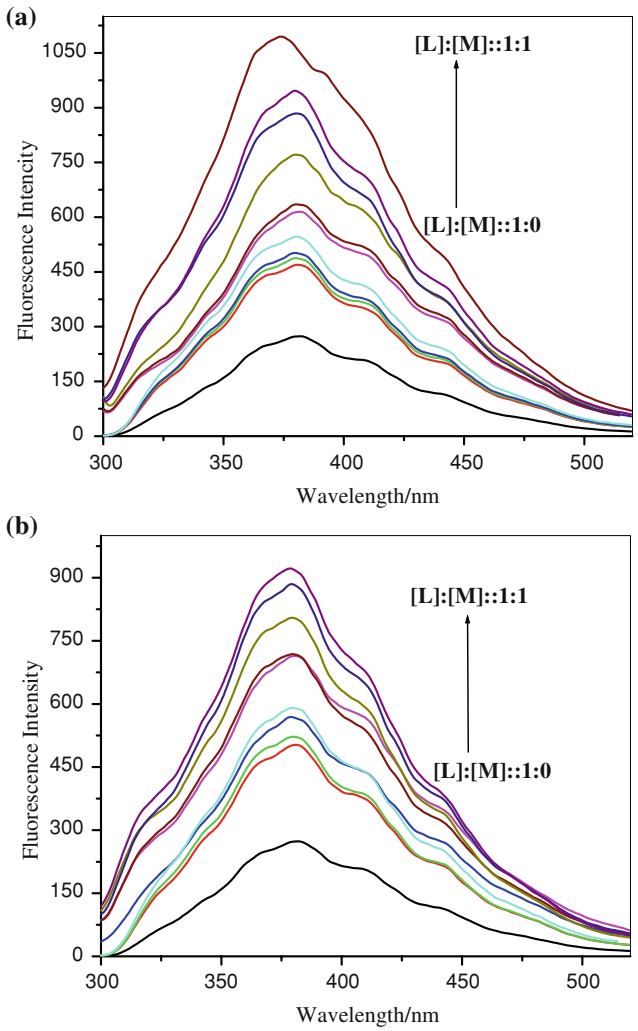

Fig. 13 Fluorescence enhancement of BABD on successive addition of **a** Cu(II) and **b** Ni(II) ions at pH 9.0, λ_{ex} = 283 nm

Conclusion

The newly synthesized ligand BABD coordinates to Co(II), Ni(II), Cu(II), and Zn(II) ions in aqueous medium at low pH through the bipyridyl N-atoms. The coordination behaviour of the ligand with Cu(II) and Ni(II) changes with increasing pH; these two metal ions translocate from the bipyridyl site to the dioxotetraamine coordination site. Significant fluorescence enhancement was observed for BABD in the presence of Cu(II) and Ni(II) at pH 9.0 in

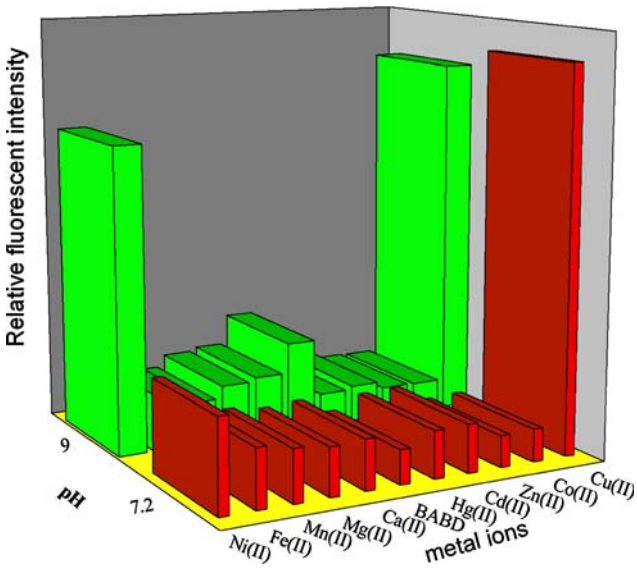

Fig. 14 Relative fluorescence intensity of BABD on addition of various metal cations ([M]/[L] = 1) in aqueous medium at pH 7.2 and 9.0 (λ_{ex} = 283 nm and λ_{em} = 379 nm)

aqueous solution; at pH 7.2, however, the fluorescence enhancement was observed with Cu(II) ions only. It was found that BABD can be implemented as a selective fluorescent sensor for Cu(II) ions in the presence of Ni(II), Fe(II), Mn(II), Co(II), Zn(II), Mg(II), Ca(II), and Hg(II) at pH 7.2.

Experimental

All chemicals used for synthesis of BABD were purchased from Sigma–Aldrich (St Louis, MO, USA) and were used as received. All solutions used for potentiometric, spectrophotometric, and fluorescence studies were prepared from double-distilled water. Stock solutions (0.01 M) of different metal ions were prepared from their reagent grade chloride salts purchased from Ranbaxy Chemical (Chandigarh, India). A stock solution of the ligand (0.01 M) was prepared. A carbonate-free 0.1 M KOH solution was prepared and standardized against potassium hydrogen phthalate. HCl of 0.1 M was prepared and its accurate concentration was determined by titrating with standard KOH. KCl solution (1 M) was used as electrolyte. Tris (Buffer) and Buffer-Titrisol purchased from Merck (Darmstadt, Germany) were used to maintain pH 7.2 and 9.0, respectively.

^{1}H and ^{13}C NMR spectra were recorded on a Bruker Avance II-400 spectrometer in D_2O and chemical shifts were reported relative to Me_4Si. IR (KBr pellet, 450–4,400 cm^{-1}) spectra were taken with a Perkin–Elmer Model RX-I FT-IR spectrometer. The electronic spectra were recorded on an Agilent-8453 diode array UV–Vis spectrophotometer. Elemental analysis (C, H, N) data were obtained with an Exeter Analytical CE-440 elemental analyzer and the results agreed with calculated values. The fluorescence spectra were taken on a Perkin–Elmer (LS55) luminescence spectrometer.

Synthesis of N,N′-bis(2-aminoethyl)-2,2′-bipyridine-3,3′-dicarboxamide

Binicotinic acid (BNA) was synthesized from 1,10-phenanthroline as reported elsewhere [53]. The esterification of BNA was carried out by passing dry HCl gas into a hot solution of BNA in absolute ethanol. The corresponding ester (3 g, 0.01 mol) was stirred with 20 cm^3 freshly distilled ethylenediamine at room temperature under a nitrogen atmosphere for 3 days. Excess ethylenediamine was removed by distillation under reduced pressure. The white solid obtained was washed several times with cold ethanol followed by ether and then dried in vacuo. The crude product was recrystallised from hot ethanol. Yield: 1.64 g (55%); M.p.: 155 °C; UV–Vis (H_2O, $c = 10^{-6}$ M): $\lambda_{max} = 264$, 216 nm; IR (KBr): $\bar{\nu} = 3{,}410$, 3,350, 3,276, 3,050, 2,958, 1,652, 1,578, 1,350, 1,166, 1,040, 986, 884 cm^{-1}; ^{1}H NMR (400 MHz, D_2O): $\delta = 2.50$ (t, 4H, $J = 6.21$ Hz), 3.17 (t, 4H, $J = 6.21$ Hz), 7.55 (dd, 2H, $J = 7.90$ Hz, 5.01 Hz), 8.04 (dd, 2H, $J = 7.90$ Hz, 1.50 Hz), 8.57 (dd, 2H, $J = 5.01$ Hz, 1.50 Hz) ppm; ^{13}C NMR (100 MHz, D_2O): $\delta = 39.65$, 42.21, 124.49, 131.38,137.14, 150.04, 154.16, 169.72 ppm.

Titration procedure

The apparatus used, the experimental details, the calibration techniques, and the titration procedures were as described elsewhere [54, 55]. Potentiometric titrations of the ligand in the absence and presence of metal ions Co(II), Ni(II), Cu(II), and Zn(II) were carried out at 25 ± 1 °C maintained from a double wall glass jacketed titration cell connected to a constant-temperature circulatory bath. The ionic strength was maintained to 0.1 M by addition of an appropriate amount of 1 M KCl solution. Titrations with L:M = 1:0, 1:1, and 1:2 were carried out, where for each titration 51 data were recorded in the pH range ~2 to ~11.5. The protonation constants and stability constants were calculated using the computer software Hyperquad 2000 [56]. The protonation constants of the ligand were also determined spectrophotometrically in aqueous medium. The apparatus and method used for the potentiometric and spectrophotometric titrations are similar, except a dilute solution of ligand (5×10^{-5} M) with HCl (5×10^{-4} M) was titrated with 0.1 M KOH at an ionic strength of 0.1 M KCl and 25 ± 1 °C in aqueous medium. After each adjustment of pH, an aliquot was removed and electronic spectra were recorded in the region 200–380 nm. The protonation constants from the spectral data were calculated by use of the non-linear least-squares fitting software pHAb [57]. The species distribution curves were obtained from the measured equilibrium constants using the software HySS [58].

Computational methods

All calculations were performed on a Pentium IV 3.0 GHz machine in a Windows 2000 environment using the computer software CAChe version 6.1.1 [59] and Hyperchem 7.5 [60]. The initial geometry of BABD leading to minimum strain energy was achieved by use of molecular mechanics using the MM3 force field followed by the semi-empirical PM3 self-consistent field (SCF) method, at the restricted Hartree–Fock (RHF) level. The geometry optimizations were performed by application of the steepest descent method followed by the Polak–Ribiere method with a convergence limit of 0.00042 kJ/mol and an RMS gradient of 0.0042 kJ/mol. The electronic spectrum of

BABD was calculated by use of semi-empirical methods with ZINDO and the PM3 Hamiltonian. The proposed 3D-model structures of the metal complexes were obtained first by MM3 treatment and then by applying the semi-empirical AM1/d method.

Acknowledgments One of the authors, RKB, is grateful to MHRD, New Delhi, for financial assistance.

References

1. Kawakami J, Miyamoto R, Fukushi A, Shimokazi K, Ho B (2002) J Photochem Photobiol A Chem 146:163
2. Ramachandran B, Samanta A (1998) Chem Phys Lett 290:9
3. Buhmann P, Pretsch E, Bakker E (1998) Chem Rev 98:1593
4. Kramer R (1998) Angew Chem Int Ed 37:772
5. Lehn JM (1995) Supramolecular chemistry: concepts and perspectives. VCH, Weinheim
6. Cram DJ (1992) Nature 356:29
7. Prodi L, Bolletta F, Montalti M, Zaccheroni N (2000) Coord Chem Rev 205:59
8. Bargossi C, Fiorini MC, Montalti M, Prodi L, Zaccgeroni N (2000) Coord Chem Rev 208:17
9. Gunnlaugsson T, Bichell B, Nolan C (2002) Tetrahedron Lett 43:4989
10. Castagnetto JM, Canary JW (1998) Chem Commun 203
11. Hua J, Wang YG (2005) Chem Lett 34:98
12. Fan J, Peng X, Wu Y, Lu E, Han J, Zhang H, Zhang R, Fu X (2005) J Lumin 114:125
13. Burdette SC, Walkap GK, Spingler B, Tsien RY, Lippard SJ (2001) J Am Chem Soc 123:7831
14. Kawakami J, Ohta M, Yamauchi Y, Ohzeki K (2003) Anal Sci 19:1353
15. Bargossi C, Eiorini MC, Montalti M, Prodi L, Zachheroni N (2008) Coord Chem Rev 17:32
16. Hill H, Raspin KA (1968) J Chem Soc (A) 3036
17. Chin M, Wone D, Nguyen Q, Nathan LC, Wagenknecht PS (1999) Inorg Chim Acta 292:254
18. De Santis G, Fabbrizzi L, Lanfredi AMM, Pallavicini P, Perotti A, Ugozzoli F, Zema M (1995) Inorg Chem 34:4529
19. Fabrrizzi L, Poggi A (1995) Chem Soc Rev 197
20. Santos MA, Gaspar M, Amorim MT (1999) Inorg Chim Acta 284:20
21. Fabrrizzi L, Licchelli M, Pallavicini P, Perotti A, Taglietti A, Sacchi D (1994) Angew Chem Int Ed 33:1975
22. Fabrrizzi L, Licchelli M, Pallavicini P, Taglietti A, Sacchi D (1996) Analyst 121:1763
23. De Santis G, Di Casa M, Fabrrizzi L, Licchelli M, Mangano C, Pallavicini P, Perotti A, Poggi A, Sacchi D, Taglietti A, Fabrrizzi L, Poggi A (eds) (1996) Transition metals in supramolecular chemistry, NATO-ASI Series. Kluwer, Dordrecht
24. Costa I, Fabrrizzi L, Licchelli M, Pallavicini P, Parodi L, Prodi L, Bolletta F, Montalti M, Zaccheroni N (1999) J Chem Soc Dalton Trans 1381
25. Jiang LJ, Luo QH, Duan C, Shen MC, Hu HW, Liu YJ (1999) Inorg Chim Acta 295:48
26. Jiang LJ, Luo QH, Wang ZL, Liu DJ, Zhang Z, Hu HW (2001) Polyhedron 20:2807
27. Jiang LJ, Luo QH, Xiang QX, Shen MC, Hu HW (2002) Eur J Inorg Chem 664
28. Luo QH, Zhang JJ, Hu XL, Jiang XQ, Shen MC, Li FM (2004) Inorg Chim Acta 357:66
29. Kurosaki H, Yoshida H, Fujimoto A, Goto M, Shionoya M, Kimura E, Espinosa E, Barbe J-M, Guilard R (2001) J Chem Soc Dalton Trans 898
30. Amendola V, Fabrizzi L, Mangano C, Pallavicini P, Perotti A, Taglietti A (2000) J Chem Soc Dalton Trans 185
31. Amendola V, Brusoni C, Fabrizzi L, Mangano C, Miller H, Pallavicini P, Perotti A, Taglietti A (2001) J Chem Soc Dalton Trans 3528
32. Amendola V, Fabbrizzi L, Mangano C, Miller H, Pallavicini P, Perotti A, Taglietti A (2002) Angew Chem Int Ed 41:2553
33. Fabbrizzi L, Foti F, Patroni FS, Pallavicini P, Taglietti A (2004) Angew Chem Int Ed 43:5073
34. Fabbrizzi L, Foti F, Patroni FS, Pallavicini P, Taglietti A (2004) Angew Chem 116:5183
35. Kodama M, Kimura E (1979) J Chem Soc Dalton Trans 325
36. Kodama M, Kimura E (1981) J Chem Soc Dalton Trans 694
37. Lampeka YD, Gavrish SP (2000) Polyhedron 19:2533
38. Luo QH, Zhang JJ, Hu XL, Jiang XQ, Shen MC, Li FM (2004) Inorg Chim Acta 357:66
39. Kwak OK, Kim JJ, Min KS, Kim J, Kim BG (2007) Inorg Chem Commun 10:811
40. Bazzicalupi C, Bellusci A, Bencini A, Berni E, Bianchi A, Ciattini S, Girogi C, Valtancoli B (2002) J Chem Soc Dalton Trans 2151
41. Bissell RA, de Silva AP, Gunaratne HQN, Lynch PLM, Maguire GEM, McCoy CP, Sandanayake KRAS (1993) Top Curr Chem 168:223
42. Rurack K, Resch U, Senoner M, Dahne S (1993) J Fluoresc 3:141
43. Trving H, Mellor DH (1962) J Chem Soc 5222
44. Stewart JJP, MOPAC 70, University of Bloomington, IN
45. Sahoo SK, Muthu SE, Baral M, Kanungo BK (2006) Spectrochim Acta A 63:574
46. Jiang LJ, Luo QH, Duan C, Shen MC, Hu HW, Liu YJ (1999) Inorg Chim Acta 295:48
47. Jiang LJ, Luo QH, Wang ZL, Liu DJ, Zhang Z, Hu HW (2001) Polyhedron 20:2807
48. Jiang LJ, Luo QH, Xiang QX, Shen MC, Hu HW (2002) Eur J Inorg Chem 664
49. Iyer CSP, Resbalan S (2005) J Lumin 111:121
50. Ghosh P, Bhardwaj PK, Mandal S, Sanjib G (1996) J Am Chem Soc 118:1553
51. Kaur S, Kumar S (2002) Chem Commun 2840
52. Banthia S, Samanta A (2002) J Phys Chem B 106:5572
53. Dholakia S, Gillard RD, Wimmer FL (1985) Polyhedron 4:791
54. Sahoo SK, Bera RK, Baral M, Kanungo BK (2007) J Photochem Photobiol A Chem 188:298
55. Sahoo SK, Baral M, Kanungo BK (2006) Polyhedron 25:722
56. Gans P, Sabatini A, Vacca A (1996) Talanta 43:1739
57. Gans P, Sabatini A, Vacca A (1999) Ann Chim (Rome) 89:45
58. Alderighia L, Gans P, Ienco A, Peters D, Sabatini A, Vacca A (1999) Coord Chem Rev 184:311
59. CAChe version 611 (2003), Fujitsu Limited
60. HyperChem Version 7.5, Hypercube Inc, 419 Philip Street, Waterloo, Ontario, Canada, N2L 3X2